

# Titania–Silica Mixed Oxides

## V. Effect of Sol-Gel and Drying Conditions on Surface Properties

D. C. M. Dutoit, U. Göbel, M. Schneider,<sup>1</sup> and A. Baiker<sup>2</sup>

*Department of Chemical Engineering and Industrial Chemistry, Swiss Federal Institute of Technology, ETH-Zentrum, CH-8092 Zurich, Switzerland*

Received April 23, 1996; revised August 28, 1996; accepted August 29, 1996

Mesoporous titania–silica aerogels have been prepared by an alkoxide–sol-gel process with ensuing supercritical drying which involved either semicontinuous extraction using supercritical CO<sub>2</sub> or transferring the solution–sol-gel liquid directly into the supercritical state. Surface properties of these materials were compared to those of conventionally dried titania–silica xerogel. The influence of several important preparation parameters (hydrolysis route, Ti-content, and drying method) on surface properties of the gels were investigated by temperature-programmed reaction and desorption (TPRD) of isopropanol and X-ray photoelectron spectroscopy (XPS). The information gained by these surface-sensitive methods was interpreted in the light of previous bulk structural investigations, i.e., X-ray diffraction, FTIR, FTRaman, and UV-vis spectroscopy. Up to 723 K, three TPRD peaks were identified and assigned to the different surface species in titania–silica mixed oxides found in previous structural investigations: inactive silica domains, titania domains, and highly dispersed Ti in silica (Si–O–Ti linkages). The Ti-containing surface species catalyzed dehydration of isopropanol to propene at different temperatures. Depending on the dispersion and nature of titanium oxo species on the surface of the titania–silica sol-gel mixed oxides (Si–O–Ti heteroconnectivity), significant differences in the reaction-desorption profiles were observed. Prehydrolysis of the silicon alkoxide had no influence on the relative abundance of Si–O–Ti connectivity inferred from FTIR. However, XPS and TPRD revealed that the Ti-concentration on the surface increased when prehydrolysis had been applied. An increase in the bulk titania content of the mixed oxides resulted in a concomitant rise in both the surface Ti/Si ratio and the relative contribution of Si–O–Ti linkages. All titania–silica gels showed enrichment of the surface with silica. This behavior strongly depended on the drying procedure applied. Low-temperature supercritical drying and evaporative drying yielded higher titania surface concentration (lower Si enrichment) compared to high-temperature supercritical drying. © 1996 Academic Press, Inc.

<sup>1</sup> Present address: F. Hoffmann-La Roche Ltd., CH-4070 Basel, Switzerland.

<sup>2</sup> To whom correspondence should be addressed. Fax: ++41/1/632 11 63.

## INTRODUCTION

Recently it has been shown that mesoporous titania–silica mixed oxides, highly active for the epoxidation of olefins, can be prepared using the solution–sol-gel (SSG) technique combined with ensuing supercritical drying (1–4). The influence of sol-gel parameters and drying conditions on the chemical, structural, and textural properties of the resulting titania–silica mixed oxides was studied using different analytical methods, including XRD, FTIR, FTRaman, thermal analysis, and N<sub>2</sub> physisorption (1). The catalytic behavior of these binary mixed oxides in epoxidation of various bulky olefins (2) and specifically isophorone (3) was investigated. Different sol-gel parameters (acid amount, hydrolysis route, ageing, and titania content) were varied in order to optimize the structural and chemical properties of the titania–silica material for use as epoxidation catalyst (4).

The analytical methods used provided a detailed characterization of the titania–silica mixed oxides and revealed pertinent relations between the preparation conditions, resulting solid properties, and catalytic performance. FTIR analysis of the generic band at ca. 950 cm<sup>-1</sup> provided an estimate of the relative abundance of Si–O–Ti connectivity, which was found to correlate well with the catalytic activity of the titania–silica mixed oxides in the epoxidation of different olefins, including cyclohexene, norbornene, cyclododecene, limonene, and isophorone (2). Compared to the bulk properties, however, relatively little is known so far about the surface properties of the titania–silica mixed oxides.

Temperature-programmed reaction and desorption (TPRD) has recently proved to be a potent tool for the surface characterization of titania–silica systems (5, 6). Biaglow *et al.* (5) showed that the selective adsorption of isopropanol is useful to discriminate between titania and silica surface domains. Dehydration of isopropanol to propene preferentially occurred on titania. By means of FTIR spectroscopy, Liu *et al.* (6) found that unitary titania contains Lewis acid sites, whereas mixed titania–silica possesses

predominantly Brønsted acid sites. The aim of this work was to extend our previous studies to the surface properties of the titania-silica mixed oxides. The influence of crucial sol-gel parameters (hydrolysis method, titania concentration) and drying conditions (evaporative drying resulting in xerogels, supercritical drying yielding aerogels) on the surface properties are investigated by TPRD of isopropanol in conjunction with X-ray photoelectron spectroscopy (XPS).

## EXPERIMENTAL

A set of acronyms is used throughout this work. The first numeral displays the nominal Ti-content in wt%, based on the theoretical system  $\text{TiO}_2\text{-SiO}_2$  (2 wt% " $\text{TiO}_2$ "  $\rightarrow$  1.5 at% Ti; 5 wt%  $\rightarrow$  3.8 at%; 10 wt%  $\rightarrow$  7.7 at%; 20 wt%  $\rightarrow$  15.8 at%); the subsequent two capital letters represent the drying method used (low-temperature supercritical drying  $\rightarrow$  *LT*; high-temperature supercritical drying  $\rightarrow$  *HT*; xerogel  $\rightarrow$  *X*), and *p* stands for prehydrolysis.

### Synthesis of Materials

The wet-chemical preparation procedure used and the findings concerning sol-gel reactivities are described in detail in Ref. (1). In brief, tetraisopropoxytitanium(IV) (TIPOT) was chemically modified with acetylacetonate (acac) (7). Modified TIPOT and tetramethoxysilicon(IV) (TMOS) were dissolved in isopropanol (i-PrOH). The hydrolysant added consisted of doubly distilled water and hydrochloric acid (HCl 37 wt%). The corresponding molar ratios of doubly distilled  $\text{H}_2\text{O}$  : alkoxide : hydrochloric acid were 5 : 1 : 0.09. As to the *two-stage* preparation (*prehydrolysis*), acidic hydrolysant was added to TMOS, leading to a hydrolysis level of 2. The modified TIPOT was added in a second step and "completion" of the hydrolysis was achieved by addition of the residual amount of doubly distilled water.

Three different drying methods were applied (1).

(i) Conventional drying (xerogels): The titania-silica gel was evaporatively dried at a pressure of 10 kPa and a temperature of 313 K for 22 h and at 373 K for another 24 h.

(ii) High-temperature supercritical drying (high-temperature aerogels): The SSG product was transferred into an autoclave. The high-pressure system was flushed with nitrogen, pressurized to 10 MPa, hermetically closed, and heated at 1 K  $\text{min}^{-1}$  to 533 K. After thermal equilibration the pressure was isothermally released at 0.1 MPa  $\text{min}^{-1}$ .

(iii) Semicontinuous extraction with supercritical carbon dioxide (low-temperature aerogels): The titania-silica gels were transferred into an autoclave and stirred by a turbine stirrer (ca. 60 rpm). At a temperature of 313 K, the autoclave was pressurized with supercritical  $\text{CO}_2$  to 24 MPa. The solvent of the SSG product was semicontinuously extracted

by a  $\text{CO}_2$  flow of 20 g  $\text{min}^{-1}$  for 5 h. Finally, the  $\text{CO}_2$  was isothermally released at a rate of ca. 20 g  $\text{min}^{-1}$ .

Portions of the uncalcined (raw) aerogel or xerogel powder were calcined in a tubular reactor with upward flow. To remove most of the organic residues prior to calcination, all aerogels and xerogels were first pretreated in a nitrogen flow of 0.5  $\text{dm}^3 \text{min}^{-1}$  at 673 K for 1 h. After cooling to ca. 353 K, they were heated at 5 K  $\text{min}^{-1}$  in air flowing at 0.5  $\text{dm}^3 \text{min}^{-1}$  and kept for 5 h at 673 K.

The composition was generally calculated on the basis of the nominal amounts used and independently confirmed by inductively coupled plasma atomic emission spectroscopy (ICPAES).

### Physicochemical Characterization

*Nitrogen physisorption.* Textural properties were determined by nitrogen physisorption at 77 K using a Micromeritics ASAP 2000 instrument. Evaluation and measurement procedures are reported in more detail in Ref. (1).

*Temperature programmed reaction and desorption.* TPRD experiments with i-PrOH (Riedel-de Haen, extra pure) were performed in a quartz tube fixed-bed microreactor with 4 mm inner diameter. Desorbing and product gases were analyzed on line by a quadrupole mass spectrometer (Balzers, QMG420 with QMA120). The reactor bed consisted of 30–80 mg sample, depending on the bulk density, with a bed height of ca. 5 mm. Prior to the TPRD runs, the samples were pretreated in an  $\text{O}_2\text{-Ar}$  flow (7 v%  $\text{O}_2$ ) at 673 K, cooled to 303 K, and purged with pure Ar (99.999%, Pan Gas). During the adsorption procedure, the sample was exposed to an Ar flow saturated with i-PrOH at room temperature. The gas flows always amounted to 50 ml (STP)  $\text{min}^{-1}$  and the time of exposure was one hour per step. After purging with Ar for 1 h, the desorption spectra were recorded by heating the sample at 10 K  $\text{min}^{-1}$  to 723 K in an Ar flow and simultaneously measuring the ion intensities of the desorbed species by mass spectrometry. The monitored ion intensities were  $\text{C}_2\text{H}_4\text{OH}^+$  ( $m/z=45$ , from i-PrOH),  $\text{C}_3\text{H}_5^+$  ( $m/z=41$ , from i-PrOH and propene), and  $\text{OH}^+$  ( $m/z=17$ , from water). The time elapsed between the desorption of a species from the sample surface and the detection was estimated to be 30 s. The Ar background was subtracted, the lowest intensity of each ion was set to zero, and the intensities were referred to either the sample mass (reference samples) or the BET surface area (all other samples).

*XPS analysis.* XPS analysis was performed in a Leybold LHS 11 instrument.  $\text{MgK}\alpha$  radiation (240 W) was used to excite photoelectrons, which were detected with the analyzer operated at 31 eV constant pass energy at a scale calibrated versus the  $\text{Au}4f_{7/2}$  at 84.0 eV. Under these conditions the full-width at half-maximum (FWHM) of the argon-ion-cleaned  $\text{Ag}3d_{5/2}$  line was 0.9 eV. Corrections of the energy

shift, due to the steady-state charging effect, were accomplished taking the C1s line at 285.0 eV, resulting from the adsorbed hydrocarbons.

## RESULTS

### Temperature Programmed Reaction and Desorption

TPRD measurements on amorphous silica (Aerosil, Degussa) and titania (P25, Degussa, consisting of 70% anatase and 30% rutile) reference samples are presented in Fig. 1. With silica no significant reaction of *i*-PrOH was observed. The coinciding ion intensity maxima of  $m/z=45$  and 41 were consequently assigned to *i*-PrOH desorption ( $\alpha$ -peak). In contrast, titania was catalytically active and showed a maximum dehydration rate of *i*-PrOH at ca. 534 K, indicated by the maxima in the ion intensity  $m/z=41$  corresponding to propene ( $\gamma$ -peak). This peak was accompanied by a peak  $m/z=17$ , indicating simultaneous water evolution (not shown). Based on these reference measurements the  $\alpha$ -peak and the  $\gamma$ -peak were attributed to silica- and titania-type surfaces, respectively. In addition to titania P25, a high-surface-area titania aerogel (8), consisting of crystalline anatase and amorphous domains, was investigated. The BET surface area of this sam-

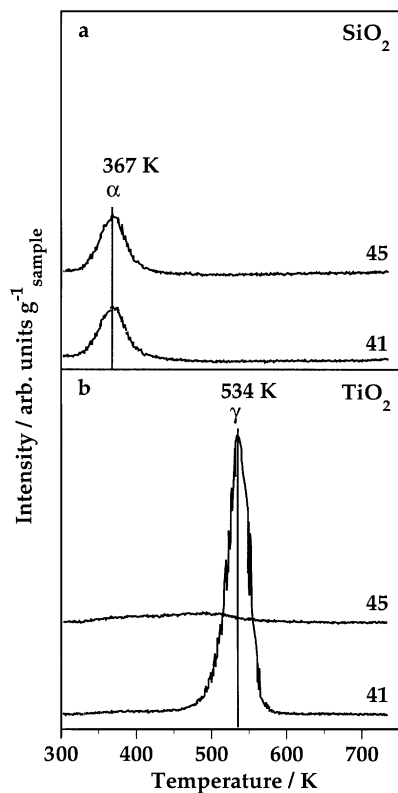


FIG. 1. TPRD measurements with *i*-PrOH on (a) amorphous silica (Aerosil, Degussa) and (b) titania P25 (Degussa) reference samples. Conditions are given under Experimental.

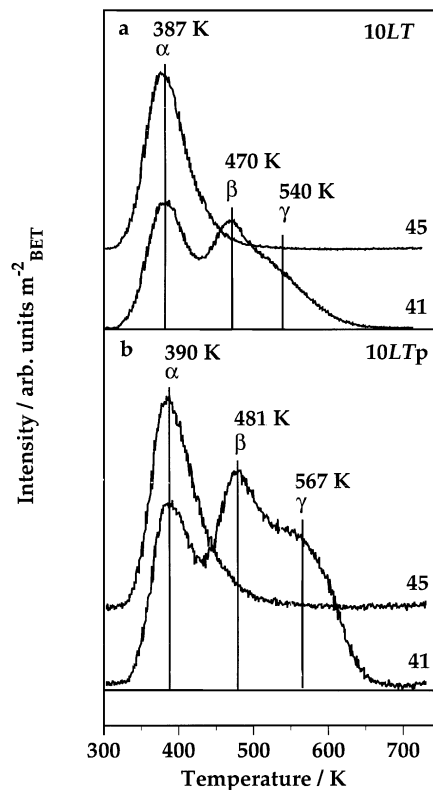
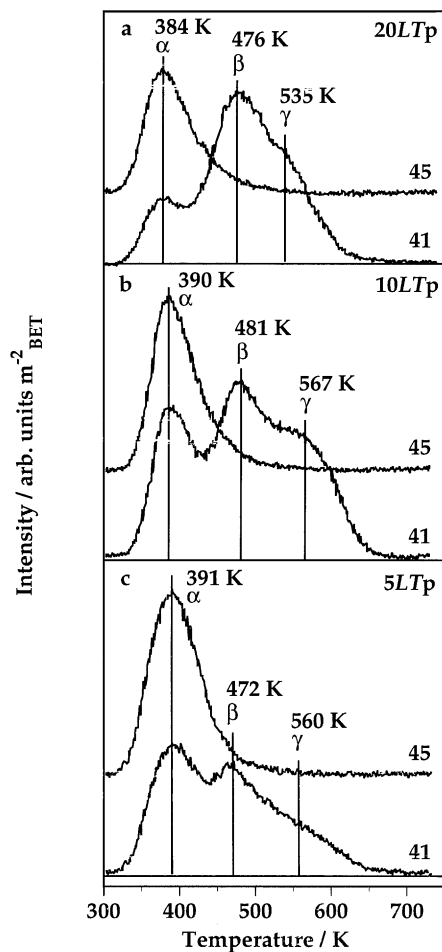


FIG. 2. Influence of prehydrolysis on the surface properties of low-temperature (*LT*) titania-silica aerogels with 10 wt% nominal  $\text{TiO}_2$ , represented by TPRD measurements with *i*-PrOH. Sample prepared (a) without prehydrolysis (10*LT*) and (b) with prehydrolysis (10*LTp*). Both samples were calcined in air at 673 K. Conditions and designations of samples are explained under Experimental.

ple was about four times higher ( $195 \text{ m}^2 \text{ g}^{-1}$ ) than that of P25 ( $50 \text{ m}^2 \text{ g}^{-1}$ ). The corresponding  $\gamma$ -peak intensity was also four times higher, suggestive of a linear correlation between  $\gamma$ -peak intensity and titania surface area. Moreover, the measurements on the different titania samples revealed that the crystallographic phase did not influence the TPRD behavior significantly.

The TPRD profiles of low-temperature (*LT* and *LTp*) titania-silica aerogels Figs. 2–4 show three discernible peaks  $\alpha$ ,  $\beta$ , and  $\gamma$ . Previous structural investigations of the *LT* titania-silica aerogels by means of UV-vis, FTIR, and XRD indicated that these materials contain Ti in two different forms, namely as highly dispersed Ti, forming Si-O-Ti linkages and as small domains of  $\text{TiO}_2$  embedded in the silica matrix. In agreement with this finding the TPRD profiles of these samples indicate that two structurally different sites contribute to *i*-PrOH dehydration to propene. Based on the reference TPRD measurements on  $\text{SiO}_2$  and  $\text{TiO}_2$  (Fig. 1) and the XPS results described later on, the  $\beta$ -peak (Figs. 2–4) was assigned to highly dispersed Ti (Si-O-Ti linkages) and the  $\gamma$ -peak to small domains of  $\text{TiO}_2$ , present as imperfections in the titania-silica aero- and xerogels.



**FIG. 3.** Influence of titania content on the surface properties of *LTp*-aerogels investigated by means of TPRD with *i*-PrOH. (a) *LTp*-aerogel with 20 wt% nominal “TiO<sub>2</sub>,” (b) *LTp*-aerogel with 10 wt% “TiO<sub>2</sub>,” and (c) *LTp*-aerogel with 5 wt% “TiO<sub>2</sub>.” The samples were all prepared with prehydrolysis step and calcined in air at 673 K. Conditions and designations of samples are explained under Experimental.

These assignments were used to assess the influence of different preparation parameters on the surface properties of titania–silica aerogels and a xerogel.

The influence of prehydrolysis on the TPRD profiles is presented in Fig. 2. The low-temperature aerogels 10*LT* and 10*LTp* with 10 wt% nominal “TiO<sub>2</sub>” exhibited  $\alpha$ -,  $\beta$ -, and  $\gamma$ -peaks. In order to estimate the  $\gamma$ -peak position, the TPRD spectra were deconvoluted into Gaussian curves. Note that the intensities of the  $\beta$ - and  $\gamma$ -peaks, referred to the BET surface area, were markedly higher for the prehydrolyzed sample. This behavior was also found for the low-temperature aerogels containing 5 wt% “TiO<sub>2</sub>” (5*LT* and 5*LTp*).

TPRD profiles of low-temperature aerogels with different titania contents (20*LTp*, 10*LTp*, 5*LTp*) are shown in Fig 3. The maxima of the  $\alpha$ -,  $\beta$ -, and  $\gamma$ -peaks are within the same range, independent of the titania contents. The  $\beta$ -peak

increases with the titania content. The  $\beta$ -peak intensity of the aerogel 20*LTp* with 20 wt% “TiO<sub>2</sub>” is almost two times higher than that of 5*LTp* with 5 wt% “TiO<sub>2</sub>” (Fig. 3). 20*LTp* exhibits the smallest  $\alpha$ -peak (assigned to silica), while 5*LTp* exhibits the smallest  $\gamma$ -peak (assigned to titania). The BET surface areas of 10*LTp* and 20*LTp* were in the same range (683 and 674 m<sup>2</sup> g<sup>-1</sup>, respectively), whereas the surface area of 5*LTp* was 518 m<sup>2</sup> g<sup>-1</sup>.

The effect of the different drying procedures on the TPRD profiles of samples containing 10 wt% nominal TiO<sub>2</sub> is presented in Fig. 4. The high-temperature aerogel (10*HT*), low-temperature aerogel (10*LT*), and xerogel (10*X*) gave rise to  $\alpha$ - and  $\gamma$ -peaks, indicative of silica and titania domains, respectively. However, only the TPRD profiles of the samples dried at low temperature (10*LT* and 10*X*) show  $\beta$ -peaks. The  $\gamma$ -peak of 10*X* occurs at higher

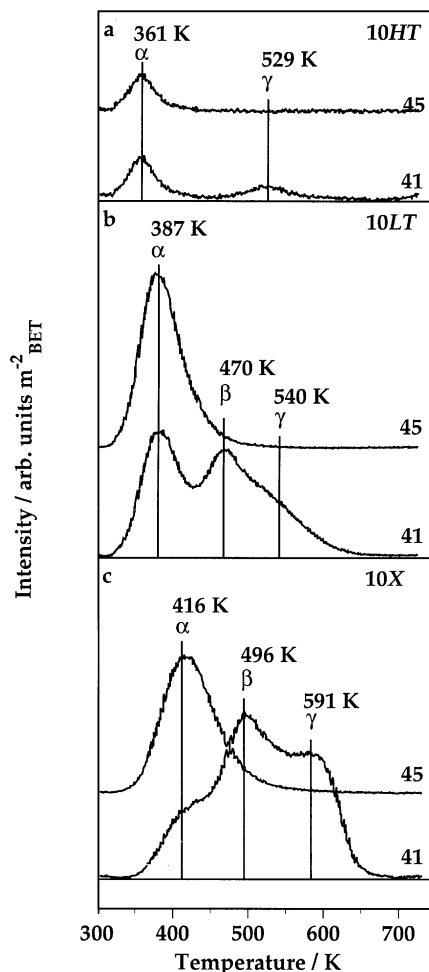


**FIG. 4.** Influence of different drying procedures on the surface properties of titania–silica samples (10 wt% TiO<sub>2</sub>), investigated by TPRD with *i*-PrOH: (a) supercritically dried high-temperature aerogel 10*HT*, (b) low-temperature aerogel 10*LT* extracted with supercritical CO<sub>2</sub>, and (c) evaporatively dried xerogel 10*X*. All samples were calcined in air at 673 K. Conditions and designations of samples are explained under Experimental.

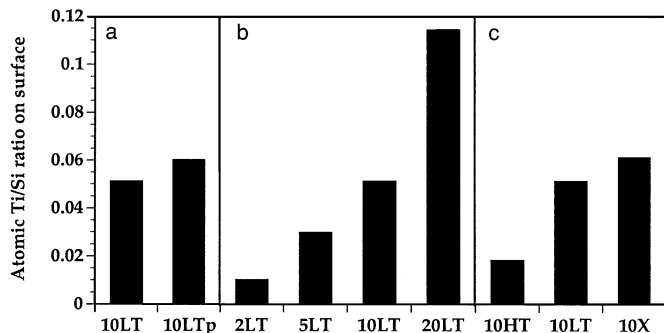


FIG. 5. Ti/Si ratio on the surface of different titania-silica samples, determined by XPS analysis: (a) low-temperature aerogel 10LT and corresponding sample 10LTp prepared with pre-hydrolysis step, (b) low-temperature aerogels with titania contents in the range 2–20 wt% nominal “TiO<sub>2</sub>”, and (c) high-temperature aerogel 10HT, low-temperature aerogel 10LT, and evaporatively dried xerogel 10X. All samples were calcined in air at 673 K. Conditions and designations of samples are explained under Experimental.

temperature compared to 10LT and 10HT. 10HT shows the weakest peak intensities. 10LT possesses the strongest  $\alpha$ -peak, and 10X possesses the strongest  $\beta$ - and  $\gamma$ -peaks among the three differently dried samples. The BET surface areas of 10HT, 10LT, and 10X were 598, 683, and 473 m<sup>2</sup> g<sup>-1</sup>, respectively.

### XPS Analysis

XPS was used to determine the Ti/Si ratio on the surface of the aero- and xerogels. Fig. 5a shows the effect of prehydrolysis on the resulting Ti/Si ratio. 10LT without prehydrolysis had a lower titania concentration on the surface than the corresponding prehydrolyzed sample 10LTp. For both samples, the bulk Ti/Si ratios of 0.083 were higher than the corresponding surface Ti/Si ratios (10LT, 0.051; 10LTp, 0.060). It emerges from Fig. 6 that prehydrolysis did not influence the maximum binding energy at 460.2 eV, which was assigned to tetrahedrally coordinated Ti in a silica matrix by Anpo *et al.* (9), Carati *et al.* (10), and Stakheev *et al.* (11). A

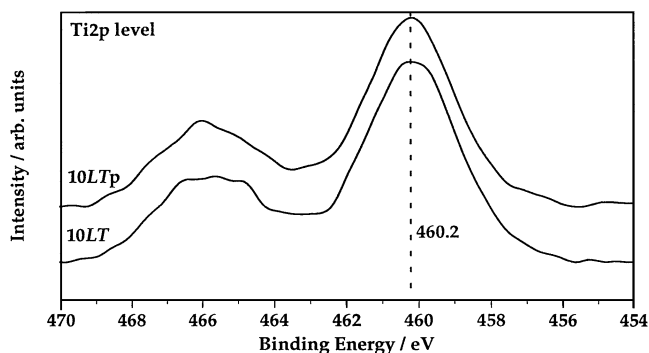


FIG. 6. XP spectra of the Ti2p level of low-temperature aerogel 10LT and corresponding sample 10LTp prepared with prehydrolysis. Both samples were calcined in air at 673 K.

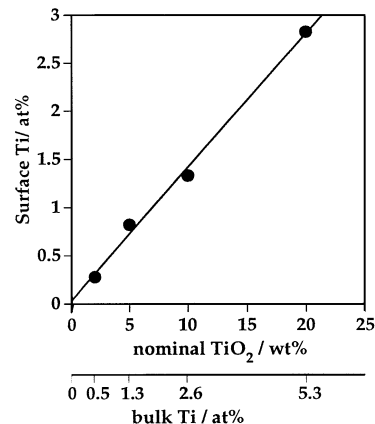


FIG. 7. Surface versus bulk concentration of Ti in LT titania-silica aerogels with 2, 5, 10, and 20 wt% TiO<sub>2</sub>, respectively. Surface concentration (at%) determined by XPS is plotted versus nominal TiO<sub>2</sub> content (wt%). Second x-axis displays bulk Ti-content in at% based on Ti-, Si-, and O-atoms. All samples were calcined in air at 673 K. Conditions and designations of samples are explained under Experimental.

slightly lower binding energy, 459.8 eV, was assigned to this species by Trong On *et al.* (12). This behavior indicated that the nature of titania surface species is similar, irrespective of the hydrolysis route chosen.

The surface Ti/Si ratios measured for low-temperature aerogels with Ti-contents in the range 2–20 wt% nominal TiO<sub>2</sub> are depicted in Fig. 5b and the comparison between surface and bulk concentration is represented in Fig. 7. The Ti-concentration on the surface increased with higher “TiO<sub>2</sub>”-content. The bulk Ti-concentration was always higher than the corresponding surface concentration (Fig. 7).

The effects of the different drying procedures on the Ti/Si ratio are shown in Fig. 5c. The theoretical Ti/Si ratio on the surface is 0.083 for a sample with 10 wt% “TiO<sub>2</sub>.” All samples investigated, 10HT, 10LT, and 10X, showed distinctly lower values in the range 0.018–0.061. Compared to the high-temperature aerogel with only ca. 20% of the bulk Ti-concentration on the surface, gels dried at low temperature (10LT and 10X) possessed ca. 70%. Consequently all samples revealed enrichment of silica on the surface. The Ti2p spectra measured for all differently dried samples are presented in Fig. 8. The binding energy of sample 10HT agrees well with the literature data for pure anatase with octahedrally coordinated Ti (458.5 eV) (13).

## DISCUSSION

### Influence of Prehydrolysis and Ti-Content

In general, the positive partial charge of titanium in the alkoxide precursor is significantly higher than that of silicon in the related alkoxide, which enhances the sol-gel activity of titanium over that of silicon (1). This property often

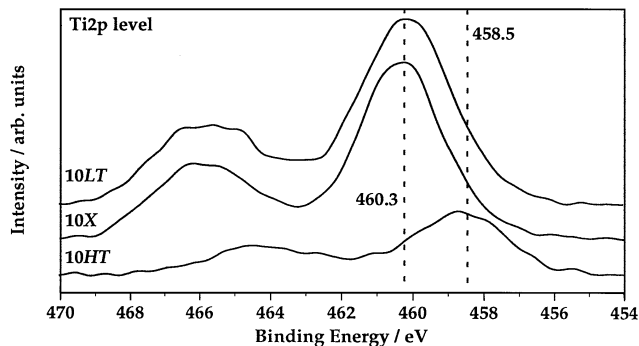


**FIG. 8.** XP spectra of the  $Ti2p$  level of differently dried titania–silica samples: low-temperature aerogel 10LT, evaporatively dried xerogel 10X, and high-temperature aerogel 10HT. All samples were calcined in air at 673 K.

results in a “core–shell” structure with titania forming the “cores.” Prehydrolysis restrains this effect by surrounding the silica sol particles built up during prehydrolysis by titania. Nevertheless the titania surface concentration of 10LTp prepared via prehydrolysis was distinctly lower than that expected from the bulk composition (theoretical Ti/Si ratio of 0.083).

Prehydrolysis increased the Ti/Si ratio on the surface (Fig. 5a), whereas Si–O–Ti connectivity, derived from FTIR analysis (1), remained almost unaffected (Figs. 2 and 6). TPRD profiles of the prehydrolyzed aerogels showed higher intensity than that of the corresponding samples prepared without prehydrolysis (Fig. 3). The shift of the peak temperatures of LTp aerogels to higher temperatures is probably a result of this (14).

LT-aerogels with Ti-contents in the range 2–20 wt% “TiO<sub>2</sub>” showed a linear increase in the surface Ti-concentration (Fig. 7). The slope (ca. 0.5) of the linear function indicates a distinct silica enrichment on the surface. This behavior supports the “core–shell” model, where the more reactive titania precursor forms the “cores.”

The TPRD profiles of LTp aerogels, shown in Fig. 3, indicate that the  $\beta$ -peak intensity increases with increasing Ti-content. This behavior is in agreement with the findings from the FTIR measurements reported in Ref. (1), where the Ti-dispersion in the silica matrix, represented by  $D_{(Si-O-Ti)}$ -values, decreased with increasing Ti-content of the sample, whereas the “absolute” contribution of Si–O–Ti connectivity ( $S_{(Si-O-Ti)}/S_{(Si-O-Si)}$ ) increased. Thus, a rise of the Ti-content favored the formation of Ti–O–Ti structural units, which even grew to titanium oxo nanodomains, as independently shown by UV–vis spectroscopy in Ref. (2). This tendency is also confirmed by the i-PrOH TPRD measurements, where the  $\gamma$ -peak intensity per surface area (assigned to titania, Fig. 1) increases with higher titania content (Fig. 3).

It is interesting to compare this result with that of other investigations. Miller *et al.* (15) found for their titania–silica

aerogels that the proportion of acid sites (sites/area) increased with both higher titania content and prehydrolysis, which is fully supported by our TPRD (Fig. 2) and XPS analysis (Fig. 5b). Sohn *et al.* (16) studied the continuous dehydration of i-PrOH in a pulse microreactor at 453 K over coprecipitated titania–silica mixed oxides. They reported that the catalytic activity per surface area increased with a rise in titania content, which is in agreement with the findings in Refs. (1, 2) and the TPRD profiles in Fig. 3.

As concerns the XPS findings, it was shown (11, 17, 18) that the O1s line shifted to lower binding energies with a rise in titania content. This observation was explained by the concomitant change from tetrahedral to octahedral coordination of Ti which reflected the increasing formation of Ti–O–Ti linkages (13). However, Stakhev *et al.* (11) measured this shift only when the concentration was increased from 10 to 50 wt% TiO<sub>2</sub>. Thus, it is not surprising that 20LT with the highest Ti-concentration on the surface (13.5 wt% TiO<sub>2</sub>) did not show any shift or line broadening of O1s.

Ingo *et al.* (18) fitted their O1s spectra with several signals by a routine applying a function of 1/2 Gaussian and 1/2 Lorentzian. They deconvoluted a spectrum of a sample with a titania content of 10 wt% TiO<sub>2</sub> in three curves assigned to Ti–O–Ti, Si–O–Ti, and Si–O–Si. The corresponding signals attributed to Ti–O–Si and Ti–O–Ti were very weak. Our spectra, however, could not be deconvoluted by the same fitting procedure. In order to exclude experimental factors being responsible for the single signal observed, the resolution of our apparatus was tested using a physical mixture of 50 wt% amorphous titania (19) and 50 wt% silica (20). We obtained two distinct signals with a difference in the binding energy of 4.1 eV. Consequently, a sufficient resolution was achieved in our measurements. Thus the lack of any shift or line broadening confirmed the high distribution of Ti in the silica matrix.

### Influence of Drying Method

In our previous studies we have shown that the use of different drying methods resulted in significant changes of the textural properties, Ti-dispersion, and crystallinity (1). The TPRD and XPS investigations allowed us to gain more information about the influence of the drying method on the surface properties.

XPS and i-PrOH TPRD showed that the xerogel 10X possessed the highest Ti-concentration at the surface among the differently dried samples (10X, 10LT, 10HT; Figs. 4 and 5c), as represented by the smallest  $\alpha$ -peak and the largest  $\gamma$ -peak. The  $\beta$ -peak intensities for highly dispersed Ti are in agreement with the  $D_{(Si-O-Ti)}$ -values, representing a relative measure of dispersion in the silica matrix (1). These  $D_{(Si-O-Ti)}$ -values decreased for the uncalcined samples in the following order: xerogel 10X (6.8), low-temperature aerogel 10LT (6.3), and high-temperature aerogel 10HT (1.5). Moreover, the dispersion values correlated well with

the activity of the titania-silica mixed oxides in the epoxidation of different olefins (2).

Bernal *et al.* (21) investigated the dehydration of *tert*-butanol, a reaction similar to that used in this work, on titania-silica gels. They determined the catalytic activity per surface area for titania-silica high- and low-temperature aerogels, xerogel, and titania-grafted silica. It is interesting to note that their reaction rates followed the same tendency as the  $\beta$ -peak intensities from *i*-PrOH TPRD in this work. They reported that the reaction rate decreased in the following order: xerogel, low-temperature aerogel, high-temperature aerogel, and grafted sample. However, in their work the difference between the samples dried at low temperature was quite small.

The above-mentioned XPS investigation of a physically mixed titania/silica sample showed that the Ti2*p* signal of amorphous titania appeared at 459.2 eV, as reported by Murata (22) for crystalline TiO<sub>2</sub>. Thus, the crystallinity of titania does not affect the position of the Ti signal. The shift of the Ti2*p* binding energy for the high-temperature aerogel 10HT (Fig. 8) reflects the segregation-agglomeration of the titania constituent induced by accelerated ageing at elevated temperature (23).

### CONCLUSIONS

TPRD measurements with isopropanol in conjunction with XPS analysis have been applied for characterizing the surface properties of titania-silica aerogels and xerogel prepared by the solution-sol-gel method. The influence of the preparation parameters, hydrolysis method, titania content, and drying route on the surface properties of titania-silica materials has been investigated. In general, isopropanol TPRD results and XPS analysis both confirmed and extended our previous findings obtained by XRD, FTIR, FTRaman, and UV-vis spectroscopy. All titania-silica gels exhibited significantly lower Ti/Si ratios at the surface compared to those in the bulk, indicative of significant silicon enrichment at the surface. Prehydrolysis increased the Ti/Si ratio on the surface, whereas the Si-O-Ti connectivity derived from FTIR remained virtually unaffected. A rise in the Ti-content of low-temperature aerogels, in the range 2–20 wt% nominal TiO<sub>2</sub>, led to an increase in both Ti-concentration and Si-O-Ti heterolinkages on the surface. As to the drying method applied, high drying temperature resulted in segregation-agglomeration of titania. The TPRD and XPS studies of the low-temperature

aerogels and xerogel not only supported the significance of the FTIR analysis for the semi-quantitative assessment of Si-O-Ti heteroconnectivity but also enabled a qualitative characterization of the nature of titania surface species.

### ACKNOWLEDGMENTS

Financial support of this work by the "Kommission zur Förderung der Wissenschaftlichen Forschung" and F. HOFFMANN-LA ROCHE AG, Switzerland, is gratefully acknowledged.

### REFERENCES

1. Dutoit, D. C. M., Schneider, M., and Baiker, A., *J. Catal.* **153**, 165 (1995).
2. Hutter, R., Mallat, T., and Baiker, A., *J. Catal.* **153**, 177 (1995).
3. Hutter, R., Mallat, T., and Baiker, A., *J. Catal.* **157**, 665 (1995).
4. Dutoit, D. C. M., Schneider, M., Hutter, R., and Baiker, A., *J. Catal.*, **161**, 651 (1996).
5. Biaglow, A. I., Gorte, R. J., and Srinivasan, S., *Catal. Lett.* **13**, 313 (1992).
6. Liu, Z., Tabora, J., and Davis, R. J., *J. Catal.* **149**, 117 (1994).
7. Aizawa, M., Nosaka, Y., and Fujii, N., *J. Non-Cryst. Solids* **128**, 77 (1991).
8. Schneider, M., and Baiker, A., *J. Mater. Chem.* **2**, 587 (1992).
9. Anpo, M., Nakaya, H., Kodama, S., Kubukawa, Y., Domen, K., and Onishi, T., *J. Phys. Chem.* **90**(8), 1633 (1986).
10. Carati, A., Contarini, S., Millini, R., and Bellussi, G., *Mat. Res. Soc. Ext. Abstr.* (EA-24), **47** (1990).
11. Stakheev, A. Y., Shpiro, E. S., and Apijok, J., *J. Phys. Chem.* **97**, 5668 (1993).
12. Trong On, D., Bonneviot, L., Bittar, A., Sayari, A., and Kaliaguine, S., *J. Mol. Catal.* **74**, 233 (1992).
13. Slinkov, W. E., and Degroot, P. B., *J. Catal.* **68**, 423 (1981).
14. Monti, D. M. A., and Baiker, A., *J. Catal.* **83**, 323 (1983).
15. Miller, J. B., Johnston, S. T., and Ko, E. I., *J. Catal.* **150**, 311 (1994).
16. Sohn, J. R., Jang, H. J., Park, M. Y., Park, E. H., and Park, S. E., *J. Mol. Catal.* **93**, 149 (1994).
17. Mukhopadhyay, S. M., and Garofalini, S. H., *J. Non-Cryst. Solids* **126**, 202 (1990).
18. Ingo, G. M., Padeletti, G., Diré, S., and Babonneau, F., *Mater. Res. Soc. Symp. Proc.* **346**, 421 (1994).
19. Dutoit, D. C. M., Schneider, M., and Baiker, A., *J. Porous Mater.* **1**, 165 (1995).
20. Dutoit, D. C. M., Schneider, M., Fabrizioli, P., and Baiker, A., *Chem. Mater.* **8**, 734 (1996).
21. Bernal, S., Calvino, J. J., Cauqui, M. A., Rodriguez-Izquierdo, J. M., and Vidal, H., *Stud. Surf. Sci. Catal.* **91**, 461 (1995).
22. Murata, M., Wakino, K., and Ikeda, S., *J. Electron Spectrosc. Relat. Phenom.* **6**, 459 (1975).
23. Schneider, M., and Baiker, A., *Catal. Rev.-Sci. Eng.* **37**(4), 515 (1995).